

# Mullite formation in clays and clay-derived vitreous ceramics

W.E. Lee<sup>\*</sup>, G.P. Souza<sup>1</sup>, C.J. McConville, T. Tarvornpanich<sup>2</sup>, Y. Iqbal<sup>3</sup>

*Department of Materials, Imperial College London, S Kensington Campus, London SW7 2AZ, UK*

Available online 8 April 2007

## Abstract

Recent studies of mullite formation in clays and clay-based vitreous ceramic systems are reviewed. In such systems, mullite crystals grow in a viscous aluminosilicate liquid, as primary 2:1 mullite in pure clays and as more acicular secondary 3:2 mullite in the presence of alkali fluxes. The stoichiometry of the mullite formed is difficult to determine since the crystals are embedded in an aluminosilicate glass matrix. However, it is likely the mullites formed have a range of Al/Si ratios as the *local* liquid composition varies significantly due to the heterogeneity of the microstructure. More fluid (fluxed with alkali and iron oxides) aluminosilicate liquids encourage growth of mullite crystals as does firing in oxidising atmosphere due to reducing atmosphere causing formation of Fe metal so removing the fluxing iron oxides from the aluminosilicate melt.

© 2007 Elsevier Ltd. All rights reserved.

**Keywords:** Mullite; Clay; Vitreous Ceramics; Porcelain; Stoneware

## 1. Introduction

Traditional, high-volume, vitreous ceramics such as white-ware, some refractories and structural clay products, in which substantial amounts (30–70) vol.% of viscous liquid forms on firing, are commonly derived from triaxial mixtures of clays, fluxes and fillers. The function of the clays, which typically are about a half of the batch, is to act as a binder for the other body constituents in the green state and to confer plasticity on the body for shaping. Kaolinite  $\text{Al}_4[\text{Si}_4\text{O}_{10}](\text{OH})_8$  is the most common clay used. The flux is about one-quarter of the batch and provides low melting phases which lower the temperature of liquid formation and react with other constituents forming liquid which permeates the microstructure leading to densification. Common fluxes include many alkali feldspars such as nepheline syenite ( $\text{KAlSi}_3\text{O}_8$  and  $\text{Na}_3\text{KAl}_4\text{Si}_4\text{O}_{16}$ ). The final quarter of the batch is filler such as quartz or alumina which is reasonably stable at commercial firing temperatures and reduces distortion and shrinkage. Mullite forms in vitreous ceramics from the clay and its interaction with the other components of the microstructure, and is believed to have

important effects on mechanical properties due to its interlocking, acicular morphology and the stress generated in the glassy matrix due to the expansile nature of its formation mechanism.<sup>1,2</sup>

The morphology, stoichiometry and composition of mullites are a complex function of the starting materials and processing route.<sup>3,4</sup> It is believed that  $3\text{Al}_2\text{O}_3 \cdot 2\text{SiO}_2$  mullite only forms directly by solid state reaction of oxide precursors and only loses  $\text{SiO}_2$  so indirectly becoming  $2\text{Al}_2\text{O}_3 \cdot \text{SiO}_2$  mullite at very high temperatures.  $2\text{Al}_2\text{O}_3 \cdot \text{SiO}_2$  mullite itself only forms directly from (e.g. melt-derived) liquid-containing systems. Sol-gel processed mullites can form directly as a single phase or can form by reaction of diphasic mixtures of  $\text{SiO}_2$  and  $\text{Al}_2\text{O}_3$ . Schneider et al.<sup>5</sup> highlight that differences in the sol-gel precursor types in terms of the scale of homogeneity and distribution of Al and Si species are key to understanding the final mullite stoichiometry and morphology. They defined three types of mullite precursors. Type I precursors are amorphous in the as-prepared state and yield mullite as the only crystalline phase at about 980 °C. Type II precursors contain pseudo-boehmite and non-crystalline silica in the as-prepared state. Pseudo-boehmite transforms to spinel phase above ~400 °C and to mullite above ~1250 °C. Type III precursors are also amorphous in the as-prepared state but partially convert to spinel phase above ~980 °C yielding mullite above ~1100 °C.

Mullite formation from clay systems is often complicated by the presence of impurities in the natural materials. How-

<sup>\*</sup> Corresponding author.

<sup>1</sup> Present address: Vitreous Materials Laboratory, Federal University of Sao Carlos, Sao Carlos, Brazil.

<sup>2</sup> Present address: University of Sheffield, UK.

<sup>3</sup> Present address: Department of Physics, University of Peshawar, Pakistan.

ever, there is basic understanding of the clay decomposition and phase crystallisation sequence with disagreement only in the fine detail.<sup>6</sup> Mullite derived from the firing of the clay component in whiteware bodies is termed *primary* mullite since it is the first to form whereas that formed from interaction of the clay component and any fluxes (typically alkali-rich feldspars) is termed *secondary*. On firing, the kaolinite mineral dehydroxylates at 500–600 °C, forming metakaolin, which consists of the kaolinite lattice after the removal of most of the hydroxyl groups. Transmission electron microscope (TEM) studies of this transformation reveal that the characteristic pseudo-hexagonal morphology of the kaolinite crystals is retained by the metakaolin, e.g.<sup>7,8</sup> As heating proceeds, a spinel-type phase crystallizes within the metakaolin, beginning at around 900 °C. This has been reported by some researchers<sup>9,10</sup> to be a  $\gamma$ -Al<sub>2</sub>O<sub>3</sub> spinel phase with some residual amorphous SiO<sub>2</sub>, and by others<sup>11</sup> as a single phase containing more Si and having a composition nearer to mullite. Mullite itself also begins to form at this stage, and the development of these phases continues to 1000 °C. TEM analysis of kaolinite fired to this temperature shows 5–10 nm crystals of spinel-type phase identifiable by electron diffraction, and primary mullite crystals on the 10–30 nm scale.<sup>7,12</sup> Amorphous, Si-rich material is also visible at this temperature, having developed from the metakaolin. At about 1100–1200 °C, spinel is lost, and elongated mullite crystals up to 0.5  $\mu$ m long begin to develop. By 1300 °C, cristobalite begins to form from the amorphous Si-rich phases, until eventually mullite and cristobalite are the only crystalline phases remaining in the body.

There have been comparatively few studies of microstructural evolution on firing illite and smectite group clays but it is generally accepted that illites dehydroxylate between 350 and 600 °C, and that the original crystal structure as observed by XRD is maintained until 700 °C. This is in contrast to kaolinite, in which the XRD reflections are lost upon dehydroxylation below 500 °C. The relict illite structure breaks down between 700 and 850 °C, and liquid phases begin to form. The octahedral portion (containing aluminium, magnesium, and iron) of the illite structure then crystallizes to form a spinel, which increases in crystal size until above 1100 °C and melts by 1300 °C. The tetrahedral part of the illite structure combines with any alkalis present to form a liquid phase, beginning at 950 °C. Mullite only begins to crystallize at 1100 °C. Smectite clays such as montmorillonite dehydroxylate below 600 °C and, as in the illites, form a stable dehydroxylated phase that retains some of the crystal structure of the original clay mineral.<sup>13</sup> The characteristic crystal structure is generally lost above 800 °C.<sup>14</sup> A spinel-type phase crystallizes from 850 °C and melts between 1100 and 1300 °C. A silica-rich liquid is formed, beginning at around 800–850 °C, from the silica tetrahedra of the original lattice and any alkalis present, and cristobalite crystallizes above 1000 °C. Mullite crystallization begins at 1050 °C.

Examination of mullite stoichiometry from clays is complicated by its being surrounded by an aluminosilicate glass matrix so making energy dispersive spectroscopy (EDS) analysis difficult. Nonetheless, it is believed that 2:1 (primary) mullite

derives from decomposition of clays while 3:2 (secondary) mullite forms from interaction of clay with fluxes.<sup>2</sup> Rezaie et al.<sup>15</sup> compared mullite evolution from kaolinite, kaolinite with added alumina and from sol–gel boehmite and colloidal silica precursors and found that dense ceramics derived from the clay contained elongated tabular mullite in a glassy matrix while those from the colloidal precursors were more equiaxed with some glass located mainly at triple junctions. Djemai et al.<sup>16</sup> studied the effect of iron oxide addition <10 wt.% on mullite recrystallisation in iron-rich kaolin and found that at 1050 °C the quantity of mullite formed increases whereas >1250 °C the growth of mullite crystals was enhanced. Soro et al.<sup>17</sup> used Mossbauer spectroscopy and X-ray diffraction (XRD) Rietveld refinement to show that Fe contributes to the structural reorganisation during mullite nucleation from iron-containing kaolinite fired 900–1250 °C. Fe substituted for octahedral Al increasing the orthorhombic *c* parameter. The quantity of structural Fe attains a saturation level with >5 wt.% Fe<sub>2</sub>O<sub>3</sub> for Fe/Al between 0.3 and 0.4 depending on the crystallinity of the kaolinite. Poorly-crystallised kaolinites show faster nucleation and growth of mullite whereas well-crystallised kaolinites nucleated mullite more slowly although followed by rapid growth favouring Fe incorporation.

This review will describe recent studies carried out predominantly at the University of Sheffield, UK into the microstructures and microstructural evolution of a series of clays and clay-based vitreous ceramics which give insight into the impact of vitreous liquids on mullite formation. They are mostly based on interrupted quench studies with suitable time/temperature profiles determined via differential thermal analyses using XRD for phase analysis and optical, scanning and transmission electron microscopies for microstructural characterisation augmented by EDS in the scanning electron microscopy (SEM) and TEM. In particular, EDS in the TEM has been used to determine the composition of glassy phases throughout microstructures, to highlight its variation and the impact of the liquid from which they are formed, on crystal morphology and evolution.

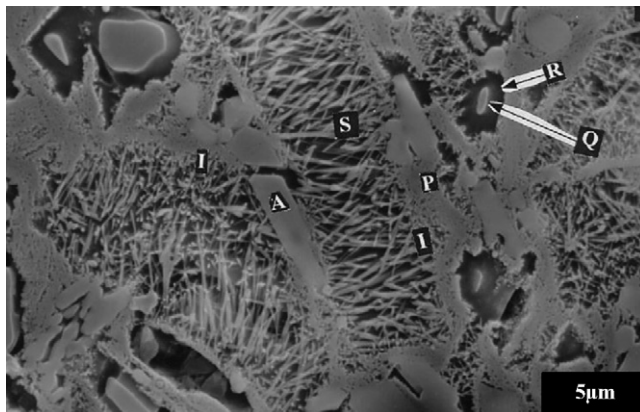


Fig. 1. Microstructure of commercial porcelain. Reprinted from Iqbal and Lee<sup>2</sup> with permission of Blackwell Publishing.

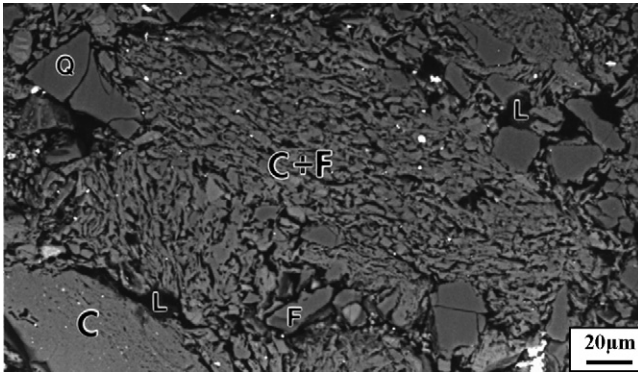


Fig. 2. Microstructure of model porcelain quenched after 3 h at 1100 °C showing pure clay C and feldspar-penetrated C+F relict agglomerates. Dark-contrast suggests liquid L formation from the flux melting, rounding of the flux crystals F and cracking of quartz Q filler are also shown. Reprinted from Iqbal and Lee<sup>20</sup> with permission of Blackwell Publishing.

## 2. Mullite in porcelains

The microstructures of commercial porcelains (e.g. Fig. 1) comprise large filler particles of alumina (A) or quartz (Q) which have started to dissolve illustrating the so-called dissolution rim (R) of highly-pure silica glass dissolving from the pure quartz crystal. These are embedded in a vitreous matrix system containing primary (P) and secondary (S) mullites. Primary mullite, formed directly from the clay decomposition has a fine, cuboidal or scaly morphology whereas the secondary mullite arises from melting of the feldspar and its reaction with the clay and has an acicular morphology. Additionally, in aluminous porcelains nanoscale tertiary mullite has been observed precipitating from alumina-rich liquid adjacent the alumina filler.<sup>1</sup> Quench studies (Fig. 2) reveal in the SEM a complex heterogeneous microstruc-

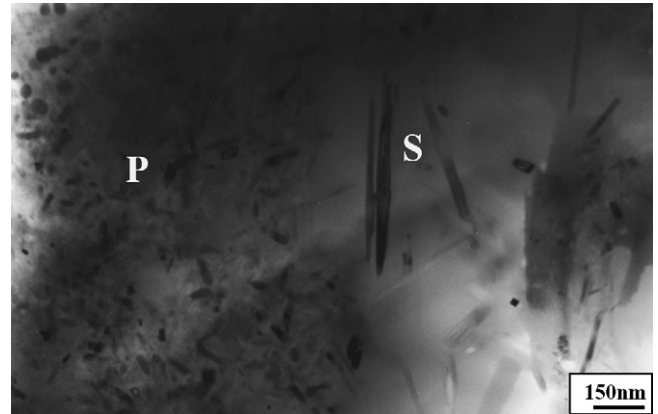


Fig. 3. Bright-field TEM of primary P on left side and secondary S mullites on the right side in model porcelain sample quenched after 3 h at 1100 °C. Reprinted from Iqbal and Lee<sup>20</sup> with permission of Blackwell Publishing.

tural evolution on firing that arises from incomplete mixing and agglomeration of the original starting materials.<sup>18,19</sup> Various regions are observed which may be clay-rich (C), or clay/flux mixtures (C+F, Fig. 2). TEM (Fig. 3) reveals the cuboidal, sometimes termed scaly, nanoscale primary (P) mullite and elongated secondary (S) mullite. EDS shows higher K<sub>2</sub>O in the aluminosilicate glass in regions of secondary mullite consistent with its derivation from alkali-rich flux reacting with the clay.

Iqbal and Lee<sup>20</sup> defined three distinct types of mullite evolving in clay-based ceramic microstructures. Type I mullite (MI) is the nanoscale <0.1 μm cuboidal primary mullite derived from clay relicts. Feldspar-penetrated clay relicts contain secondary, elongated Type II mullite (MII) <1 μm long and also occasional highly acicular elongated up to 20 μm long Type III (MIII) mullite needles. EDS chemical analysis of mullite embedded in an aluminosilicate glass matrix is difficult and data must be

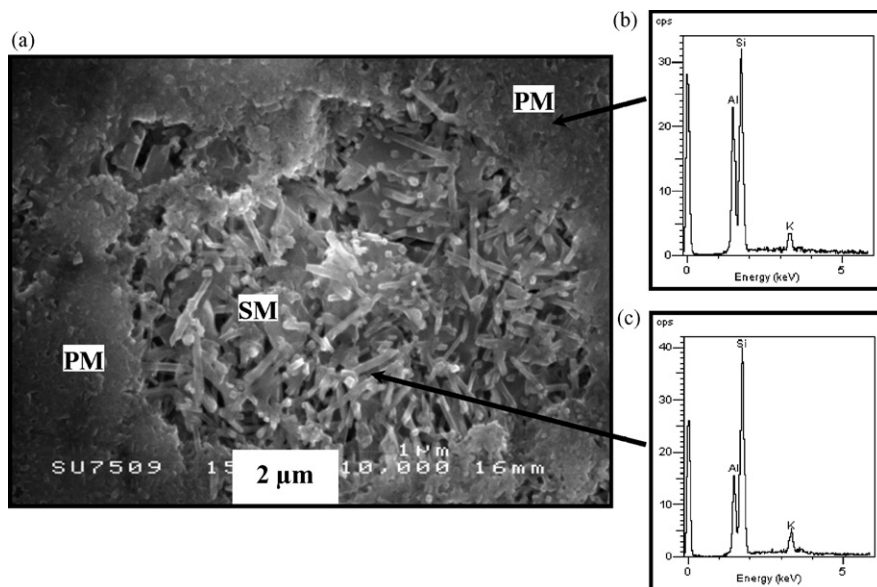


Fig. 4. SEM/SE image of cross-sectioned, etched kaolin clay pellets fired 3 h at 1200 °C. (a) Mullite particles; (b and c) EDS of primary mullite PM and secondary mullite SM. From reference [21].

treated with caution due to overlap of glass and crystal analysis. Nonetheless, semiquantitative EDS revealed that the  $\text{Al}_2\text{O}_3$  content for primary MI mullite was higher than for secondary MII and MIII mullite consistent with the idea that primary mullites are  $\sim 2:1$  mullite whereas secondary mullites are richer in silica in flux penetrated regions where fluid aluminosilicate liquid is available and so are nearer  $\sim 3:2$  mullite. In most cases, the glass close to quartz grains contained  $\text{SiO}_2$  only, whereas the potassium aluminosilicate glass composition varied in the matrix throughout the microstructure and contained up to 13 wt.%  $\text{K}_2\text{O}$  in some regions containing secondary mullite. This is consistent with the size and shape of the mullites formed. The mullite is more acicular and longer going from Types MI to MII to MIII mullite due to the increasingly fluid alkali-rich silicate liquid in which it is located enhancing crystal growth.<sup>19</sup> It is worth noting that even primary mullite becomes acicular after extended times at temperature.

### 3. Mullite in pure clays

Since clays are natural minerals they contain various levels of impurities including, significant for mullite formation, alkalis and Fe-containing compounds. Furthermore, different types of clays contain different species especially alkalis actually within their crystal structures which exude and lead to more fluid silicate liquids on firing. Such compositional variation means that the distinction between ostensibly primary and secondary mullites can become blurred and has led to some confusion in the literature. Clearly, distinguishing clay-derived primary mullite from alkali-fluxed secondary mullites in such systems can be troublesome and in such cases the terms primary and secondary become pretty meaningless. Fig. 4 from Tarvornpanich<sup>21</sup> shows the microstructure of an ECC International Ltd. Cornwall, UK kaolin clay containing 2.98 wt.%  $\text{K}_2\text{O}$ , 0.27 wt.%  $\text{Na}_2\text{O}$ , 0.1 wt.%  $\text{CaO}$  and 0.28 wt.%  $\text{MgO}$  impurity fired 3 h at  $1200^\circ\text{C}$  revealing it to contain primary and secondary mullite. SEM (Fig. 4a) shows scaly primary and rod-like  $\sim 1\text{--}2\ \mu\text{m}$  long secondary mullite. The chemical composition EDS in Fig. 4b and c of the two mullite types is different. The scale-like crystals are higher in Al but lower in K compared to the rod-like ones. This difference in shape is explained by the formation of primary mullite in the area once rich in clay and the formation of rod-like mullite in the area containing impurities such as muscovite and K-feldspar, which is the source of potassium and can act as flux to facilitate the liquid formation on firing, allowing crystallisation of longer crystals. The EDS also reveals the primary to be nearer  $2:1$  mullites and the secondary nearer  $3:2$  although the higher Si content in the secondary mullite crystals could arise from the glassy matrix in which it is embedded. It thus is apparent that the distinction between  $2:1$  and  $3:2$  mullites in these vitreous systems is blurred because the compositions can vary across the whole range of stoichiometry depending in large part on what elements are available in the local environment. There is also a trend to move from  $2:1$  to  $3:2$  mullite with increasing temperature, presumably due to alumina loss to or silica gain from the aluminosilicate glass matrix.

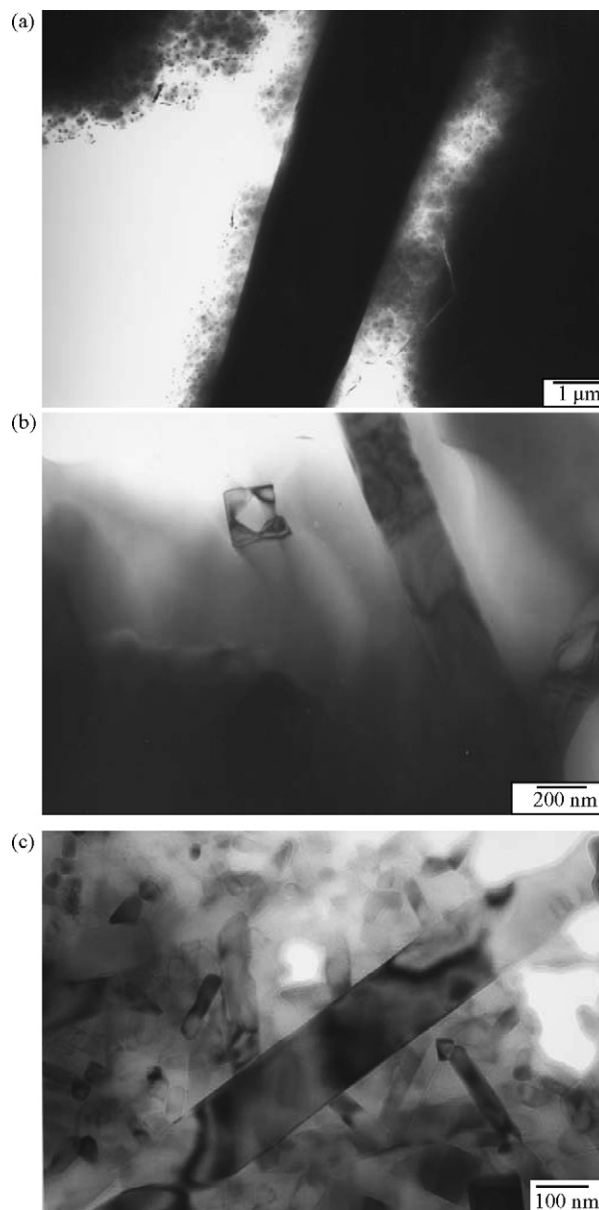


Fig. 5. BF TEM images of mullite formed from (a) illite fired 3 h at  $1400^\circ\text{C}$ ; (b) montmorillonite fired to  $1300^\circ\text{C}$  and (c) kaolinite fired 3 h at  $1400^\circ\text{C}$ . From McConville<sup>22</sup>.

McConville<sup>22</sup> examined mullite formation from three highly pure kaolinite  $\text{Al}_4[\text{Si}_4\text{O}_{10}](\text{OH})_8$ , illite  $\text{K}_{1.5}\text{Al}_4[\text{Si}_{6.5}\text{Al}_{1.5}\text{O}_{20}(\text{OH})_4]$  and smectite  $\text{Ca}_{0.33}[\text{Al}\cdot\text{Mg}]_4\text{Si}_8\text{O}_{20}(\text{OH})_{4-x}\cdot x\text{H}_2\text{O}$  clays. Mullite derived from each clay grew to very different sizes after similar heat treatments (Fig. 5, note the different length scales) being  $>10\ \mu\text{m}$  long in the illite,  $>1\ \mu\text{m}$  in the smectite and only  $\sim 0.5\ \mu\text{m}$  long in the kaolinite. Measured by X-ray fluorescence alkali  $\text{Na}_2\text{O} + \text{K}_2\text{O}$  levels in the clays were 7.9 wt.% for the illite, 2.3 wt.% for the smectite and 0.5 wt.% impurity for the kaolinite while  $\text{Fe}_2\text{O}_3$  levels were 6.2 wt.% for the illite, 4.8 wt.% for the smectite and 0.9 wt.% for the kaolinite. The high alkali/ $\text{Fe}_2\text{O}_3$  containing and so fluid silicate liquid generated from the illite clay clearly facilitates mullite crystal growth, while the lower alkali/ $\text{Fe}_2\text{O}_3$  content of

the thus more viscous liquids generated from the smectite and kaolinite clays support growth to a lesser extent. Fe was also detected in the mullite by EDS in the TEM. Fe is well known to act as a mineraliser supporting mullite growth in clay-based systems.<sup>16,17</sup>

#### 4. Mullite in porcelain stoneware

Porcelain stoneware is the world leader in the tiling market<sup>23</sup> and has been the subject of much recent research especially into use of waste material such as recycled soda-lime-silica (SLS) glass as replacement for feldspar flux in its formulation. The high firing temperatures of porcelain stoneware >1200 °C mean that different types of waste can be incorporated while still producing an as-fired material with a level of desired microstructural heterogeneity comparable to that of its waste-free counterpart. Moreover, the high firing temperature enables some wastes to be more easily incorporated into the glassy matrix leading to enhanced properties.<sup>24</sup> A typical porcelain stoneware body formulation contains 40 wt.% illite, 1 wt.% kaolinite, 15 wt.% K-feldspar and 35 wt.% Na-feldspathic sand containing quartz. Replacement of 15 wt.% of the Na-feldspar (which contains ~18 wt.% Al<sub>2</sub>O<sub>3</sub>) with SLS glass (which contains 1.5 wt.% Al<sub>2</sub>O<sub>3</sub>) led to detectably lower contents mullite in the resulting stoneware (Souza et al.<sup>23</sup>) presumably due to the Al<sub>2</sub>O<sub>3</sub> deficiency in the aluminosilicate liquid making it more difficult for mullite to grow. While mullite content was reduced new phases formed with the SLS flux including wollastonite, sodium silicates and plagioclase solid solution between sodium and calcium aluminosilicates, the latter likely competing with mullite for Al/Si ions.

Souza<sup>25,26</sup> recently examined the use of high Fe-containing clays in stonewares. The Fe was present in the raw clay predominantly as iron hydroxides and on firing for 30 min at 1100 °C in an oxidising atmosphere (static air) as part of a model porcelain stoneware formulation (comprising 65% clay, 10% nepheline syenite and 25% fine quartz) formed into veins of haematite Fe<sub>2</sub>O<sub>3</sub> particles (Fig. 6). However, comparison of the mullite formed on firing in reducing atmosphere (5% H<sub>2</sub> and 95% Ar carrier gas) revealed significant differences. For similar heat treatments larger primary and secondary mullite crystals formed in oxidising than in reducing atmosphere (Fig. 7). The mechanism for the effect on mullite growth is believed associated with

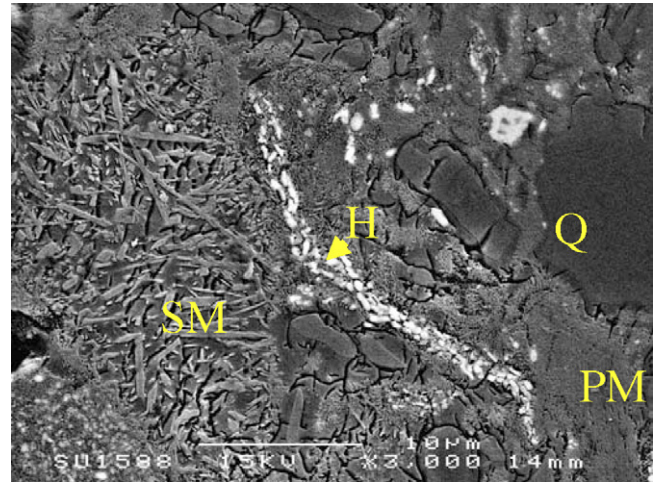


Fig. 6. Backscattered electron SEM image of a cross-sectioned, etched model stoneware composition fired in oxidising atmosphere at 1100 °C. PM: primary mullite; SM: secondary mullite; Q: quartz and H: haematite. From Souza<sup>25</sup>.

atmosphere-induced changes to the liquid composition which is likely to be more fluid in the oxidising atmosphere facilitating mass transport and crystal growth. XRD (Fig. 8) reveals Fe<sub>2</sub>O<sub>3</sub> and cristobalite formation in oxidising atmosphere but Fe metal in reducing. Removal of the fluidising iron oxides from the silicate liquid in reducing atmosphere fired samples is believed responsible. However, a contribution may be associated with the potential for transient FeO in the reducing atmosphere to mineralise quartz formation (as detected in Fig. 8) making mullite growth from silica-deficient liquid more difficult. This ability to control the extent and nature of mullite formation through control of atmosphere in cheap, abundant Fe-containing clays has significant commercial implication especially if colour control via specific Fe-compound formation is possible.

#### 5. Comments on mullite stoichiometry in vitreous systems

The stoichiometry of mullite from vitreous systems formed concomitantly with complex aluminosilicate liquids is contentious and difficult to measure. As mentioned in Section 1, mullite derived by more conventional processing is stable 3:2 formed by solid state reaction and metastable, acicular 2:1

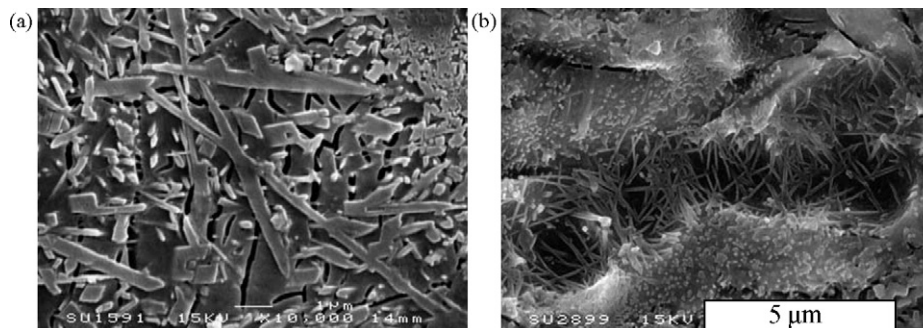


Fig. 7. Secondary electron SEM images of model porcelain stoneware compositions, polished and etched after firing 30 min at (a) 1125 °C in oxidising air atmosphere and (b) 1100 °C in reducing atmosphere. Reprinted from Souza et al.<sup>26</sup> with permission of Blackwell Publishing.

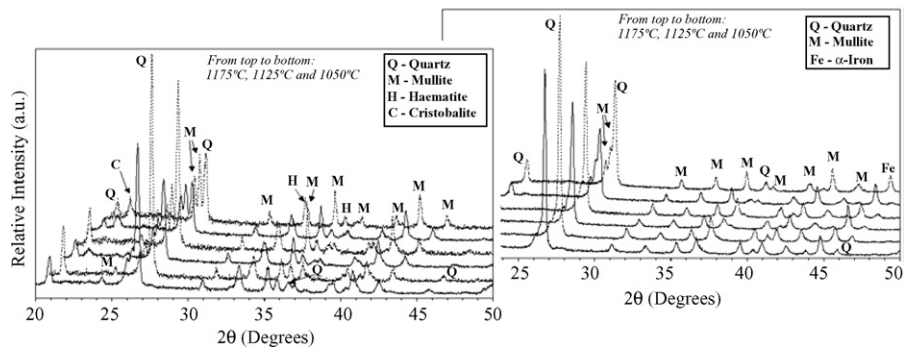


Fig. 8. XRD of specimens of model porcelain stonewares fired in oxidising left and reducing right atmosphere. Reprinted from Souza et al.<sup>26</sup> with permission of Blackwell Publishing.

formed from the melt in the presence of liquid glassy phase as expected from the commonly-accepted phase diagram of Aksay and Pask.<sup>27</sup> It is perhaps important to highlight that the observations of mullite in vitreous ceramics and clays in this study and many previous studies are on impure systems which are likely to be far from equilibrium so that simple equilibrium phase diagrams may not be relevant. The results described suggest that the general statement the primary mullite derived from pure clay is 2:1 and secondary mullites derived from clay/flux interaction are 3:2 is an oversimplification since we believe that there are a range of mullites in vitreous systems across the 2:1 to 3:2 range and the systems are not at equilibrium.

## 6. Conclusions

Mullite is seen to form in vitreous ceramics with a range of morphologies and compositions. Mullite content is controllable, e.g. by extending time and temperature. Variables affecting the mullite formation include type of flux, level of alkalis and Fe impurities and atmosphere particularly in Fe-containing systems. These variables influence mullite and other phase formation by affecting the composition and viscosity of the liquid in which it grows. The stoichiometry of mullite formed in vitreous systems is difficult to determine since the crystals are embedded in an aluminosilicate glass matrix. However, it is likely the mullites formed have a range of Al/Si ratios as the local liquid composition varies significantly due to the heterogeneity of the microstructure. Primary mullites are believed predominantly 2:1 and secondary predominantly 3:2 but the mullite compositions vary gradually and most are neither but in between, depending on the local situation, e.g. liquid composition or solid particles available for reaction.

## References

- Carty, W. M. and Senapati, U., Porcelain—raw materials, processing, phase evolution and mechanical behaviour. *J. Am. Ceram. Soc.*, 1998, **81**, 3–20.
- Iqbal, Y. and Lee, W. E., Fired porcelain microstructure revisited. *J. Am. Ceram. Soc.*, 1999, **82**(12), 3584–3590.
- Schneider, H., Okada, K. and Pask, J. A., *Mullite and Mullite Ceramics*. Wiley, Chichester, UK, 1994, p. 251.
- Lee, W. E. and Rainforth, W. M., *Ceramic Microstructures: Property Control by Processing*. Chapman and Hall, London, UK, 1994, p. 580.
- Schneider, H., Saruhan, B., Voll, D., Merwin, L. and Sebald, A., Mullite precursor phases. *J. Eur. Ceram. Soc.*, 1993, **11**, 87–94.
- McConville, C. J. and Lee, W. E., Microstructural development on firing illite and smectite clays compared with that in kaolinite. *J. Am. Ceram. Soc.*, 2005, **88**(8), 2267–2276.
- McConville, C. J., Lee, W. E. and Sharp, J. H., Microstructural evolution in fired kaolinite. *Br. Ceram. Trans.*, 1998, **97**(4), 162–168.
- McConville, C. J., Roch, G. E., Lee, W. E. and Smith, M. E., Structural evolution of clay minerals on firing deduced from solid state NMR, XRD and TEM. In *Proceedings of 10th International Ceramics Congress (CIMTEC 2002), Advances in Science and Technology, Vol. 34 Science for New Technology of Silicate Ceramics*, ed. P. Vincenzini and M. Dondi. Techna, Florence, Italy, 2003, pp. 97–108.
- Sonuparlak, B., Sarikaya, M. and Aksay, I. A., Spinel phase formation during the 980 °C exothermic reaction in the kaolinite-to-mullite reaction series. *J. Am. Ceram. Soc.*, 1987, **70**(11), 837–842.
- Onike, F., Martin, G. D. and Dunham, A. C., Time-temperature-transformation curves for kaolinite. *Mater. Sci. Forum*, 1986, **7**, 73–82.
- Srikrishna, K., Thomas, G., Martinez, R., Corral, M. P., De Aza, S. and Moya, J. S., Kaolinite-mullite reaction series: a TEM study. *J. Mater. Sci.*, 1990, **25**, 607–612.
- McConville, C., Lee, W. E. and Sharp, J. H., Comparison of microstructural evolution in kaolinite powders and dense clay bodies. *Br. Ceram. Proc.*, 1998, **58**, 75–92.
- Brett, N. H., MacKenzie, K. J. D. and Sharp, J. H., The thermal decomposition of hydrous layer silicates and their related hydroxides. *Quart. Rev. Chem. Soc.*, 1970, **24**, 185–207.
- Brindley, G. W. and Udagawa, S., High-temperature reactions of clay mineral mixtures and their ceramic properties: II, reactions of kaolinite-mica-quartz mixtures compared with the  $K_2O-Al_2O_3-SiO_2$  equilibrium diagram. *J. Am. Ceram. Soc.*, 1960, **43**(10), 511–516.
- Rezaie, H., Rainforth, W. M. and Lee, W. E., Mullite evolution in ceramics derived from kaolinite, kaolinite with added  $\alpha$ -alumina and sol-gel precursors. *Br. Ceram. Trans.*, 1997, **96**(5), 181–187.
- Djemai, A., Balan, E., Morin, G., Hernandez, G., Labbe, J. C. and Muller, J. P., Behaviour of paramagnetic iron during the thermal transformation of kaolinite. *J. Am. Ceram. Soc.*, 2001, **84**, 1017–1024.
- Soro, N., Aldon, L., Jumas, J. C., Laval, J. P. and Blanchart, P., Role of iron in mullite formation from Mössbauer spectroscopy and Rietveld refinement. *J. Am. Ceram. Soc.*, 2003, **86**, 129–134.
- Iqbal, Y., Messer, P. F. and Lee, W. E., Non-equilibrium microstructure of bone china. *Br. Ceram. Trans.*, 2000, **99**(3), 110–116.
- Lee, W. E. and Iqbal, Y., Influence of mixing on mullite formation in porcelain. *J. Eur. Ceram. Soc.*, 2001, **21**(14), 2583–2586.
- Iqbal, Y. and Lee, W. E., Microstructural evolution in triaxial porcelain. *J. Am. Ceram. Soc.*, 2000, **83**(12), 3121–3127.
- Tarvornpanich T. *Recycled colourless soda-lime-silica glass as an alternative flux in whitewares*. Ph.D. Thesis. University of Sheffield, UK, 2007.
- McConville C.J. *Related microstructural development on firing kaolinite, illite and smectite clays*. Ph.D. Thesis. University of Sheffield, UK, 1999.

23. Souza, G. P., Rambaldi, E., Tucci, A., Esposito, L. and Lee, W. E., Microstructural variation in porcelain stoneware as a function of flux system. *J. Am. Ceram. Soc.*, 2004, **87**(10), 1959–1966.
24. Tarvornpanich, T., Souza, G. P. and Lee, W. E., Microstructural evolution on firing soda-lime-silica glass fluxed whitewares. *J. Am. Ceram. Soc.*, 2005, **88**(5), 1302–1308.
25. Souza GP. *Densification behaviour and microstructural evolution of a red clay-based stoneware*. Ph.D. Thesis. University of Sheffield, UK, 2005.
26. Souza, G. P., Messer, P. F. and Lee, W. E., Effect of varying quartz particle size and firing atmosphere on densification of brazilian clay-based stoneware. *J. Am. Ceram. Soc.*, 2006, **89**(6), 1993–2002.
27. Aksay, I. A. and Pask, J. A., Stable and metastable equilibria in the system  $\text{SiO}_2\text{-Al}_2\text{O}_3$ . *J. Am. Ceram. Soc.*, 1975, **58**(11–12), 507–512.